

# We are IntechOpen, the world's leading publisher of Open Access books Built by scientists, for scientists

6,900

Open access books available

186,000

International authors and editors

200M

Downloads

Our authors are among the

154

Countries delivered to

TOP 1%

most cited scientists

12.2%

Contributors from top 500 universities



WEB OF SCIENCE™

Selection of our books indexed in the Book Citation Index  
in Web of Science™ Core Collection (BKCI)

Interested in publishing with us?  
Contact [book.department@intechopen.com](mailto:book.department@intechopen.com)

Numbers displayed above are based on latest data collected.  
For more information visit [www.intechopen.com](http://www.intechopen.com)



# Recent Advances of High Entropy Alloys: High Entropy Superalloys

*Modupeola Dada, Patricia Popoola, Ntombizodwa Mathe, Samson Adeosun, Sisa Pityana, Olufemi Aramide, Nicholas Malatji, Thabo Lengopeng and Afolabi Ayodeji*

## Abstract

This study reviews the recent technological advancements in manufacturing technique; laser surface modification and material; High Entropy Superalloys. High Entropy Superalloys are current potential alternatives to nickel superalloys for gas turbine applications and these superalloys are presented as the most promising material for gas turbine engine applications.

**Keywords:** high entropy alloys, high entropy superalloys, nickel superalloys, turbine engine, laser surface modification

## 1. Introduction

Energy transformation comprises the turbine, which is an inner combustion device and a spinning engine that utilizes water, wind steam, helium and air to produce work [1]. Kaygusuz [2] stated that dams use turbines as an electrical generator producing electricity for residential and industrial consumption. Nonetheless, in 1939, the first jet engine that powered an aircraft was built consisting of the combustion chamber, the turbine and the compressor [3]. This turbine used air as its working fluid in an internal combustion engine and this engine, in turn, removes enough chemical energy to convert it to mechanical energy from the fuel source while using the working fluid to drive the propeller and the engine [4]. Bell and Partridge [5] anticipated that the Joule cycle is a theoretical cycle for gas turbine applications, where both expansion and compression routes take place in a rotating machine [6]. This comprises some reversible processes such as the turbine using the expansion process and fluid friction for an increase in entropy which causes a spontaneous reaction using the compression method in the Brayton cycle [7]. The gas turbine is characterized by extended overhaul intervals, an increased operating speed, less moving parts, availability, low maintenance, reliability, long life span and rugged design [8]. The design of a turbine engine dictates its performance and the performance requirement are determined by the shaft house power developed in certain temperature conditions which may be extreme. Therefore, the need for high-performance materials becomes necessary because one factor which affects the efficiency of the engine; the turbine inlet temperature is made up of materials which are designed to reduce flow losses and must withstand erosion, corrosion and stress at elevated temperatures [9]. According to Reed [10],

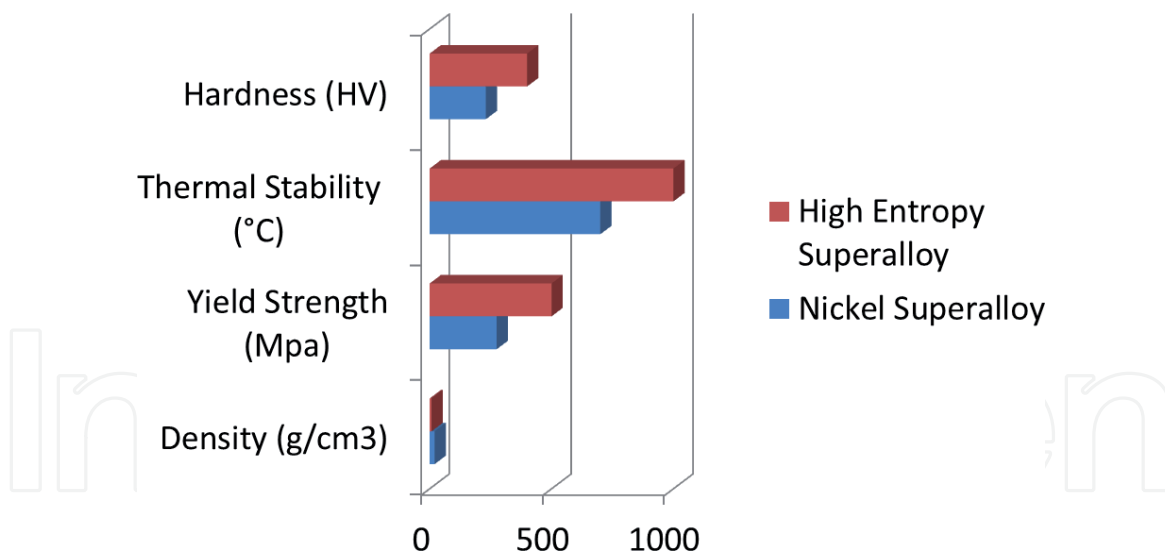


**Figure 1.**  
Comparison graph between nickel super alloy and high entropy superalloy.

superalloys especially Nickel Superalloys are materials generally used at elevated temperatures for these gas turbine applications attributed to their elevated temperature strength, corrosion resistance, excellent formability, cost and low density [11]. However, the nickel-based superalloy has a maximum service temperature, not over 650 °C attributed to the conversion of  $\gamma'$  precipitate strengthening matrix to the  $\delta$  phase over time [12]. More so, the nucleation and growth of some cavities along the transverse grain boundaries of these materials are the gas turbine airfoil's failure mechanisms [13]. Therefore; a need to develop new materials with improved properties was necessary and this was achieved by transforming conventional material into new ones via advanced industrial reproduction [14]. Miracle, Tsai [15] proposed High Entropy Superalloys (HESAs) as a new class of amalgam with superior properties compared to traditional superalloys as shown in **Figure 1**.

Their elemental composition, lower densities, high configurational entropy and core effects alongside possessing the  $\gamma'$  precipitate reinforcement phase makes this superalloy a preferred alternative material for turbine engine applications [16]. In a previous study, additive manufacturing was presented as a potential advance manufacturing technique as opposed to conventional arc melting and casting fabrication processes. This study attempts to present HESAs as a promising material for gas turbine engine applications, as opposed to traditional Nickel-based superalloys [17].

## 2. Advances in material development

### 2.1 Super alloys

Superalloys are stable materials; they do not oxidize or fall apart in very harsh environments and at high temperatures. These amalgams are used for power generation, industrial, marine and aerospace applications [10]. They are characterized by their excellent heat and oxidation resistance at elevated temperatures, high melting temperature, and high-temperature mechanical strength, good fracture toughness, and stress-rupture, creep resistance [18]. In general, superalloys contain more of Co, Ni, Cr or Fe but less of Ta, Hf, W, Cr, B, Mo, Nb, Al, Zr, C, Ti because these elements adversely affect the properties of the blend. Superalloys have a typical face-centred cubic structure and are characterized by a  $\gamma'$  precipitate with operating temperatures above 600 °C [19]. This phase gives the superalloy a

principal yield strength which increases with a temperature rise. They may have equiaxed or columnar grain structures without exhibiting high-angle grain boundaries, which at high temperatures are sites for damage accumulation [20]. According to Graybill, Li [21], Superalloy's strengthening mechanism includes dispersion strengthening, solid solution and precipitation strengthening [22]. The dispersion of chemically inert carbides and nitride enhances the strength of the superalloy. Precipitation of all intermetallic phases, namely; carbides and FCC matrix  $\gamma'$  precipitate enhances the strength of the superalloy through Ti, Nb, Ta and Al, which promote the formation of the  $\gamma'$  precipitate. Finally, solid solution strengthening with tungsten, columbium, rhenium, molybdenum, rhenium and tantalum stabilizes the FCC structure and strengthens the superalloy [23].

Gessinger and Bomford [24] suggested that Superalloys for gas turbine applications are widely fabricated using powder metallurgy. However, Bewlay, Gigliotti [25] fabricated the turbine disks using hot die forging and roll forming. Lavella, Berruti [26] studied the residual stresses in Inconel 718 turbine disks fabricated by milling while Groh, Gabb [27] developed a turbine disk using the casting technique. Compared with these conventional techniques, the powder metallurgy process produces turbine disks which are extremely difficult to forge; die life is relatively poor and die fill is extremely difficult but not with additive manufacturing.

### *2.1.1 Nickel superalloys*

Gas turbine engines require higher temperatures for efficiency. This high-temperature application, therefore, requires excellent emission control with an advance in the combustion hardware of the engine. Nickel superalloys materials were developed for this purpose and they make up about half of the weight of materials used in turbine engines [28, 29]. They have an FCC nickel matrix which is stable enough for the alloy to be used for combustion liners, blades, vanes, thermal barrier coatings, burners and are also applied to bear loads of over 75% of their emergent melting temperature. This is attributed to their characteristic high-temperature rupture and creep resistance, lifetime expectancy, low operating costs and excellent thermal efficiency [30]. Nickel superalloys are also used in space vehicles, submarines, petrochemical equipment and nuclear reactors. Nickel-based superalloy 718 (IN718) is widely used in wrought or cast at 540 °C for rotors in gas turbine applications [14]. Nickel superalloy 925 and 725 having good corrosion resistance are applied in the oil and gas industry where carbon dioxide, hydrogen sulphide, free Sulfur and chloride levels are significantly high. Nickel superalloy 706 (IN706) is used for power generation for its large diameter and lower concentrations of other alloying elements. Alloy 685 (Waspaloy) with high-temperature strength and age hardening is widely used for gas turbine engine applications [31]. The superalloy is resistant to corrosion and oxidation whilst withstanding extreme atmospheric conditions while in service. Other compositions are; Rene N6 used in Jet engines, Inconel Alloy 600 used for stills, condensers, heaters and evaporator tubes. Alloy 601 is used for pollution control, power and aerospace applications [32]. Nimonic 90 is used for turbine disc, blades, hot-working tools and forging. However, Nickel-based superalloy is difficult to machine attributed to its hardness, toughness, and they possess high heat resistance at elevated temperatures alongside low thermal conductivity [33]. Machining at high pressure causes work hardening rapidly, which invariably causes the alloy component to warp. Furthermore, Nickel superalloys can be easily replaced with alloys that have high creep strength and niobium silicide was an appropriate system to replace nickel superalloy having 170 MPa creep strength and at a density of 7 g/cm<sup>3</sup> until recently. Research showed that the addition of Ru and Re to the nickel superalloy led to the enhancement of the superalloy's creep strength,

however; these additions are expensive and cause density inversion which results in the defect [34]. This superalloy's stability is limited at very high temperatures [35].

According to Durand-Charre [36], Nickel-based Superalloys are majorly FCC phase structured. However, in aluminum-nickel superalloy systems, a second precipitate phase is formed, which is usually Ni<sub>3</sub>Al in a composition containing an ordered intermetallic structure [37]. The  $\gamma'$  phase relies on the cooling rate of the superalloy through the solvus temperature of 894 °C [38]. A fast cooling rate promotes a unimodal distribution of the  $\gamma'$  precipitate, therefore, an increasing the volume of the  $\gamma'$  phase through rapid solidification is essential to the strengthening properties of the superalloy [28]. Although the precipitate morphologies can be modified through heat treatment and other secondary phases observed in Nickel-based superalloys are ordered FCC  $\gamma'$ , FCC carbides, ordered body-centred tetragonal  $\gamma''$  and ordered orthorhombic intermetallic phases [39].

Pollock and Tin [28] did an intensive review on nickel superalloys and the authors stated that the commercial superalloys comprise Co, Cr, W, Mo, Ta, W, Nb, Re, Ti, Al, C, Hf, Y, B and Zr. The yield strength of the nickel superalloy is between 900–1300 MPa at room temperature and the fatigue life at 593 °C is 600 MPa at 10<sup>6</sup> cycles and 10<sup>9</sup> cycles. Additions of Re, Nb, W and Mo can be added for the solid solution strengthening of the superalloy. Y, Ta and Cr contribute to enhance the corrosion and oxidation properties of the superalloy. While Zr, C, Hf and B are carbides or borides forming agents that help enhances the mechanical properties of the superalloy as they are situated at the grain boundaries. The creep rupture life attains about 1100 °C at 137 MPa stress level after 1000 h which is about 90% fraction of the melting point signifying the need for innovative advanced materials having higher melting points for the hottest regions of the turbine engine.

### *2.1.2 High entropy superalloys (HESAs)*

Throughout the years, alloys utilized for commercial reasons were structured by choosing an element which framed the network of the whole component with the addition of essential solutes to the base component [40, 41]. The blends of these combinations were reduced as could reasonably be expected for the immense development of mass intermetallic mixes existing within the molar atomic proportions of these alloys, hence, attaining a 40% mark or more. Along these lines, the intermetallic phases reduce the quality of the alloys while in service [42, 43]. Therefore, a need arose to search for alloys with atomic percentages lesser than 35% and the possibilities of combining many metallic principal elements in several atomic compositions were further investigated [44]. According to Ye, Wang [45], an innovative class of alloys with these attributes was discovered more than a decade ago by mixing multiple principal elements in equimolar or near-equimolar compositions. Yeh, Chen [46] named the alloys 'High Entropy Alloys' (HEAs). The authors defined HEAs as amalgams having compositions with at least five principal metallic elements, with these components having a molar atomic proportion between 5 and 35% [47]. Studies on HEAs have concluded that most HEAs comprise simple FCC, BCC or HCP solid solutions phase attributed to their high-entropy effect [48]. Wang, Li [49] suggested that these solid solution phases with little or no intermetallic matrix enable HEAs to have outstanding properties such as strength, extraordinary mechanical and physical properties at cryogenic temperatures, plastic strain, fracture strength and good ductility; they possess elevated-temperature oxidation resistance and excellent work hardenability and have been reported to possess distinctive magnetic and tribological properties [50, 51]. Furthermore, Senkov, Wilks [52] reported that HEAs are exceptional refractory materials and their fatigue-resistance were reported to exceed conventional alloys by Hemphill [53].

In the literature, the development in the solid solution strengthening of High Entropy Alloys (HEAs) and the precipitation hardening properties of the alloys at temperatures above 1100 °C, led to the discovery of High Entropy Superalloys (HESAs). Yeh, Tsao [17] stated that these superalloys are simply HEAs with the bulk of  $\gamma'$  precipitates and they are described by their high elongation at room temperature, compressive strength, lower densities, creep resistance and ultimate tensile strengths at elevated temperatures. Tsao, Yeh [54] suggested that High Entropy Superalloy (HESA) is made up of a first elemental content containing at least 35 at.% and each principal reinforcement elemental combination will have a second elemental content of more than 5 at%, for example,  $\text{Ni}_{40.7}\text{Al}_{7.8}\text{Cr}_{12.2}\text{Fe}_{11.58}\text{Co}_{20.6}\text{Ti}_{7.2}$  HESA. Senkov, Isheim [55] developed a refractory high entropy superalloy and the authors anticipated that the first and second elemental composition content is derived by the mixing entropy of more than 1.5 R (R is the ideal gas constant) alongside the principal strengthening elemental composition, respectively.

Chen, Chang [56] studied the hierarchical microstructural strengthening of HESAs and the composition of strengthening elements can consist of Cu, Fe, Ti, Zr, Co, V, Al, Nb, Cr and Mn. While the overall structure can comprise Mn, Ni, Fe, Ti, Co, Cr and V while for the grain boundary strengthening; C, B and Hf are added but must not be over 15% of the superalloy's total compositional weight. Refractory elements like Ru, Ta, Re, Mo and W can be added but must also contain less than 15% of the total superalloy's weight [55]. Tsao, Yeh [57] in 2013 recommended the development of superalloys using HEAs microstructure with single phases and an additional second phase for elevated temperatures applications. Yeh, Tsao [17] then fabricated  $\text{Ni}_{40.7}\text{Al}_{7.8}\text{Co}_{20.6}\text{Cr}_{12.2}\text{Fe}_{11.5}\text{Ti}_{7.2}$  high entropy superalloy (HESA) via casting method. The authors reported that the microstructure of the composition was stable at elevated temperatures and the superalloy was made up of  $\gamma'$  nanosized precipitates with a density lower than 8 g/cm<sup>3</sup>.

Daoud, Manzoni [58] developed  $\text{Al}_8\text{Co}_{17}\text{Cr}_{17}\text{Cu}_8\text{Fe}_{17}\text{Ni}_{33}$  HESA using thermocalc, the authors compared the results with Alloy 800H and IN617. They reported that the HESA had higher tensile strength, this was attributed to two phases; one spherical  $\gamma'$  precipitate which was less than 20 nm after the aging temperature at 700 °C and another less than 350 nm with an elongated morphology. He, Wang [59] fabricated  $\text{Fe}_{94}\text{Co}_{94}\text{Ni}_{94}\text{Cr}_{94}\text{Ti}_2\text{Al}_4$  HESA with  $\gamma'$  nanosized precipitates to manipulate the thermomechanical properties of HESAs, and they argued that the superalloy had  $\gamma'$  nanosized precipitate with an outstanding yield strength and elongation [60]. According to Xiao, Gregoire [61], scanning alternating current calorimetry can be used to quantify the thermomechanical properties of superalloy.

Wang, Zhou [62] investigated  $\text{Al}_{0.2}\text{CrFeCoNi}_2\text{Cu}_{0.2}$  HESA and discovered the  $\gamma'$  nanosized precipitate with 30% elongation. Tsao, Yeh [57] developed seven HESAs using the elements Ni, Fe, Al, Cr, Co, Ti by vacuum arc melting. They stated that the development of the  $\gamma$  precipitates in the superalloy was due to Fe, Cr elements and the  $\gamma'$  matrix, they stated that substituting Ni with Ti enhances the thermal stability of HESAs thus encouraging the  $\gamma'$  matrix and by controlling the elemental compositional partitioning in the middle of the  $\gamma$ - $\gamma'$  phase, the thermal properties of the high entropy  $\gamma$  matrix can be improved. More so, at elevated temperatures after long term exposures  $\text{L}_{12}$   $\gamma'$  nanosized precipitates were formed without topological closed packed phases. Gwalani, Soni [63] examined  $\text{Al}_{0.3}\text{CoCrFeNi}_2$  and  $\text{Al}_{0.3}\text{CoCrFeNi}$  HESAs and the authors observed  $\gamma'$  precipitate in the  $\text{Al}_{0.3}\text{CoCrFeNi}$  super alloy until 550 °C but were replaced with a B2 phase at 700 °C after annealing attributed to the increase in aluminum content [64].

Senkov, Isheim [55] and Li, Lee [65] tested  $\text{AlMo}_{0.5}\text{NbTa}_{0.5}\text{TiZr}$  HESA by powder metallurgy and they all observed that the superalloy possessed high thermal stability and yield strength superior to nickel superalloys at 1200 °C. Kai, Cheng [66]

examined the oxidation behavior of a HESA in O<sub>2</sub> environments. The Ni<sub>2</sub>FeCoCrAl<sub>0.5</sub> HESA oxidation kinetics at 900 °C followed a parabolic-rate law forming scales which was dependent on the oxygen pressure. The results showed that the oxidation rates increased with an increase in oxygen pressure however, the kinetics of mass-loss was observed. Shafiee, Nili-Ahmadabadi [67] designed a wrought HESA using Phacomp and CALPHAD technique. The reports showed that the superalloy comprised of  $\gamma'$  nanosized precipitates with lower densities, excellent workability and high thermal stability than Inconel 718 alloy and Waspaloy. Saito, Chen [68] discussed the influence of heat treatments on HESA microstructural evolution and results showed the cast HESA had coarsened  $\gamma'$  precipitates attributed to microsegregation which decreased the solidus making the  $\gamma'$  solvus unclear. Finally, Zhang, Huo [69] prepared cast Ni<sub>48-x</sub>Co<sub>18</sub>Fe<sub>9.3</sub>Al<sub>9.7</sub>Cr<sub>10.5</sub>Ti<sub>4.5</sub>Mo<sub>x</sub> HESA to investigate the mechanical and microstructural properties of the superalloy and they concluded that HESAs exhibits good compressive strength at elevated temperature, elongation and tensile strength at room temperatures than nickel superalloy.

HESAs are stable at elevated temperatures compared with commercial Rene' N6, Udimet 700 and Hastelloy X superalloys, this attributed to their sluggish diffusion and high entropy effect. At high temperatures, Nickel-based superalloys form intermetallic topological closed-packed (TCP) phases rich in Fe-Cr because of the high iron content in less than 100 h at 900 °C and this TCP phases formed is detrimental to the stability of superalloys at high temperatures [70]. However, at 900 °C in more than 200 h, there was no TCP phase observed in Ni<sub>40.7</sub>Al<sub>7.8</sub>Cr<sub>12.2</sub>Fe<sub>11.58</sub>Co<sub>20.6</sub>Ti<sub>7.2</sub> HESA and the  $\gamma$ - $\gamma'$  microstructure of the superalloy remained stable after isothermal aging for 500 h at 1050 °C [57]. The elevated temperature strength of HESAs has been reported to be higher than that of IN 617. This can be attributed to enhancing the APB energy, increasing the lattice distortion and/or adding refractory Ta and W elements in high concentration to the compositional system.

Yeh and Tsao [71] did a thorough analysis of HESAs with the elemental composition of Fe, C, Al, Mo, Cr, Ti, Ni, Co, Ta, W and Nb. The siderophile element was Nickel while the strengthening element was Nb and C. The authors reported that the HESA's microstructure comprised an FCC, L12 crystal structure and  $\gamma'$  phase while the superalloys had hardness values of 400–470 HV at room temperature. At elevated temperatures, the HESAs hardness values recorded were between 300–350 HV. These values are greater than IN718 under high temperature. The yield strength of HESA at 1000 °C was about 500 MPa. At a strain of 150 MPa under a temperature of about 980 °C, the HESAs showed excellent elevated temperature creep strength when compared with first generational superalloys. The creep strength and fatigue resistance of HESAs is due to the positive lattice misfit of the superalloy [72]. The raft which directionally coarsens the  $\gamma'$  precipitate is corresponding with the stress axis which results in a sluggish motion of dislocation in the  $\gamma$ - $\gamma'$  precipitate interface, thus hindering the propagation of cracks initiated by fatigue and perpendicular to the same stress axis [73]. The HESAs showed promising thermal stability with a compact protection layer of Cr<sub>2</sub>O<sub>3</sub>, Al<sub>2</sub>O<sub>3</sub> observed on the surface of the HESAs at elevated temperatures, while the densities of the HESAs ranged from 7.78–7.94 g/cm<sup>3</sup> as opposed traditional superalloys that range between 7.8–9.4 g/cm<sup>3</sup> attributed to the high concentration of Cr, Fe, Ti and Al elements [42]. Other superalloys used for turbine engine applications are presented in **Table 1**.

## 2.2 Protection of superalloys in gas turbine applications

Wee, Do [81] described in a review of the mechanical thermal properties of superalloys and the authors stated that superalloys are required to perform excellently under severe thermal and mechanical stresses. The turbine engine may experience failure attributed to linear and cyclic movements of the pistons, connecting rods, rotors and

SuperAlloy	Composition	Phase Structure	Advantages	Disadvantages	Ref
Iron-Based (Incoloy 800H, Type A-286 alloy, IN903)	IN800H (32Ni-21Cr- 1.5Mn-01Si- 0.3Ti-0.3Al-01C- bal Fe, wt.%)	$\gamma$ and $\gamma'$	Room- temperature strength, high- temperature strength, Creep, Wear and oxidation resistance	Difficult to machine, poor service performance, susceptible to defects, hot corrosion degradation	[74–76]
Cobalt-Based	(Co-30Ni-11Al- 2Ti-5.5 W-2.5Ta- 0.1B, at%)	$\gamma, \gamma'$ and TCP	High strength at elevated temperatures, corrosion -resistant, thermal shock resistant, easy to machine	Low strength compared to other superalloys,	[77, 78]
Titanium- based (TiAl, Ti6Al4V)	(Ti-48Al-2Cr- 2Nb)	$\gamma$ , FCC L1 <sub>2</sub>	High Strength- toughness and fatigue strength, corrosion- resistant,	Low adhesive, high friction coefficient, low ductility	[79, 80]

**Table 1.**  
*Superalloys used for turbine engine applications.*

shafts majorly affecting the cascade fluids on the surface of the superalloy [82]. For turbine applications, superalloys comprise elements which are meant for elevated temperature strength required for efficiency [83]. However, these alloying elements may also adversely impact the superalloy's resistance when in this severe environmental conditions over some time. Therefore, there may be a need for additional protection of the superalloy through surface treatments [84]. There are several laser surface modification treatments, namely; laser surface hardening, laser surface heat treatment, Laser alloying, laser shot peening, laser surface dispersing and laser coatings and cladding [85]. Laser coatings enable the superalloy to be resistant to its environment, have microstructural stability and enhance its thermal, physical and mechanical properties [28, 86]. The coatings available can be classified as; overlay coatings, diffusion coatings and ceramic barriers [87, 88]. The deposition of Al from a different external source and diffusing it into the base superalloy to form an external layer is called aluminide or diffusion coating. Bonding an oxidation-resistant alloy which is weak but highly effective on a superalloy to enable surface protection and stability is called overlay cladding, while ceramic barriers are ceramic coatings attached to the surface of a superalloy [89].

### 3. Advances in manufacturing technology

Technological advancements in surface engineering have replaced conventional methods of surface treatments with laser surface modification (LSM) techniques. The use of lasers in LSM has been reported to produce wear, corrosion, fracture and fatigue resistant HEAs coatings. This is attributed to the energy absorption and rapid solidification of the deposition process, which promotes fine microstructures necessary for surface modification.

According to Wu et al. [90] used laser surface alloying to study the phase evolution and cavitation erosion-corrosion behavior of a HEA coating in distilled water and NaCl solution. The study showed that the alloy's cavitation erosion resistance

was enhanced in distilled water but not in NaCl solution due to the corrosion. Zhang et al. [91] fabricated HEA by laser surface alloying to examine the properties of the alloy and they reported that the microhardness property of the coating was thrice the number of the substrate and there were improvements in the wear resistance of the alloy. Huang et al. [92] investigated an equimolar HEA on a titanium alloy substrate using LSM and the results also showed enhancements in the wear resistance of the alloy attributed to the manufacturing route which contributed to the formation of the phases observed in the BCC matrix. Nahmany et al. [93] used an electron beam surface remelting technique to modify two-five component HEAs, and the authors inspected the influence of these surface modification processes on the properties of the alloys. The authors observed a significant increase in the microhardness due to the rapid solidification and cooling process associated with the fabrication technique. From literature, it can be deduced that LSM classified into laser surface remelting, surface amorphisation, laser transformation hardening, shock hardening, laser cladding, laser surface alloying and laser shock peening using different types of lasers can be used to enhance the properties of HEAs [94].

#### **4. Laser surface modification**

Laser application in surface modification techniques can be dated back to Albert Einstein who was the first scientist to conceive a stimulated emission in 1917 which today makes lasers applicable [95].

A laser is an abbreviation for “light amplification by stimulated emission of radiation”. It is classified into CO<sub>2</sub> and Excimer gaseous lasers, Nd:YAG Solid-state Lasers, Liquid Dye lasers and Yb-doped Fiber. These lasers consist of an optical resonator, a pumping energy outlet and a gain medium. The gain medium is located inside the optical resonator which amplifies a light beam using external energy supplied by the pumping energy outlet. They are classified into dyes, semiconductors or fibers, solid and gaseous states.

Lasers are generally characterized by the ability to avoid divergence in a long-distance, possession of an increased level of energy and monochromaticity [96].

- a. The CO<sub>2</sub> laser comprises an electric pump, discharge tube, CO<sub>2</sub> gas for the gain medium and optics such as silver or gold mirrors, zinc selenide lens and finally a window as the optical resonator. Although the Helium-Neon laser was the first gas laser developed in a Bell telephone laboratory, still, the CO<sub>2</sub> is the most widely used gas laser for its high emission wavelength between 9–11 μm which offers very high power for surface modification. The process experiences low light absorption in the infrared regions, reduced optical fiber delivery, instability in the output power attributed to the contraction of the laser structure and thermal expansion when pumping the gas by an AC or DC which sometimes limits its application. Zhang et al. [97] reported fabricating HEAs with CO<sub>2</sub> laser, and the alloy had fine microstructural morphologies and higher mechanical properties. While Zheng et al. [98] mentioned that the HEAs coating fabricated using gas lasers had cellular crystals with dispersion precipitates although the hardness values were reported to be high [99].
- b. Excimer lasers, on the other hand, is a mixture of noble gases like helium buffer gas, xenon, argon and a chloride or fluoride halogen. Excimer which is about 248 nm is also known as excited dimers which are pumped using a pulsed electrical discharge for the production of nanosecond pulses in an ultraviolet region, for that reason; it can only be operated in a pulsed mode. Other limitations of this laser

are low beam quality, the severity of maintenance and high running cost [100]. Sharma et al. [101] reported using an excimer laser with a wavelength of 248 nm for target ablation during the creation of epitaxial single crystal high entropy  $\text{ABO}_3$  perovskite thin films. The authors described how this process was significant in understanding different bonding environments to develop macroscopic responses driven by complex exchange interactions and electron–phonon channels.

c. Nd:Yag which is an acronym for neodymium-doped yttrium aluminum garnet laser is a 1064 nm solid-state laser made up of an active ion and a host from either glass or solid crystalline. It is one of the widely used for the surface modification of HEAs attributed to the ability of its light beam to be transported by flexible optical fibers, consequently increasing its delivery efficiency and compactness [102, 103]. It is also not limited by its mode of transport, which can occur both in pulse and continuous modes. Recently, diode lasers have been substituted for Xenon flash lamps as the pump source to improve the quality of the beam. More so, Nd:  $\text{YVO}_4$  is a recent substitute for the Nd:Yag laser due to its wider band absorption, high efficiency and lower operating threshold [104].

d. A Fiber Laser is about 848 nm in wavelength with a rare earth doped fiber used for high power generation due to its increased level of efficiency. The Yb-Doped fiber lasers have excellent electrical-to-optical efficiency with system compactness and high-quality beam. Neodymium, holmium, thulium, dysprosium, erbium and praseodymium are other rare earth elements used as a gain medium in fiber lasers. Fiber lasers are usually pumped with laser diodes; however, they are limited by their light propagation through the optical fiber which greatly influences the guiding medium compared with when the propagation occurs through the air inside the fiber. More so, other factors like the Kerr lens and Raman effects limit the performance of the laser, therefore, optical fibers with polarization maintenance are strongly recommended as the gain medium [105]. Fan et al. [106] examined the influence of fiber laser welding on the mechanical and microstructural properties in addition to the solute segregation of a high entropy alloy. The authors reported that the alloy showed dendritic structures with those fabricated using Nd:Yag laser and they observed copper's segregation to the interdendritic region were also attributed to its smaller bonding energies with other elements in the HEA composition, conversely; the alloy showed better hardness and strength compared with the Nd:Yag.

e. Organic liquid dye lasers use organic dyes as the gain medium. These liquid dye with about 50–100 nm compared to solids have a higher density of atoms and they are evenly distributed. These lasers with wide bandwidth are replaceable and are transferred from very intricate regions which are sometimes used as solutes in considerable solvents to develop gain mediums [107]. Coumarin, pyrromethene, exalite, pyridine, styryl and fluorescein are dyes used for pulsed or tunable lasers. Nevertheless, these lasers are limited in applications because they require a large volume of organic solvents for efficiency. Xu et al. [108] used a laser stimulated fluorescence equipment consisting of an organic liquid dye to fabricate a HEA and study the performance of the coatings then the influence of aluminum on the properties of the alloy. The authors stated that the laser technology and the aluminum content enabled the phase transitions, grain refinement and corrosion resistance observed.

f. Other types of lasers are; semiconductor lasers, hybrid laser arc welding and free-electron lasers and the fabrications of HEAs using these lasers are limited in research, hence, should be further explored.

#### **4.1 Laser surface melting (LSM)**

This type of surface modification is used for material hardening, electrochemical and tribological resistance and reduction in porosity. An increased rate of heat transfer occurs during the interaction between the substrate and the melted HEAs coating surface, especially during solidification. The rapid solidification and cooling rates invariably produce fine microstructures which also enhances the surface properties of the alloys. Chen et al. [109] used LSM on HEAs and they mentioned that the surface modification process increased the electrochemical and mechanical properties of the alloys. Ochelik et al. [105] found that the solidification rate influences the phases formed using LSM. The fast solidification rates promoted the BCC phase observed which was also responsible for the improved hardness properties of the alloys. Cai et al. [110] also reported observing a BCC solid solution phase and improved microhardness properties after using LSM. The as-remelted HEAs coatings had low wear mass loss showing an improvement in the wear resistance.

#### **4.2 Laser transformation hardening (LTH)**

The LTH heats the HEAs coating or films at a very high temperature with an unfocused beam, and then rapid cooling occurs immediately without letting equilibrium phases to form by quenching, as a result, generating very low thermal distortion. This method uses a diode laser or CO<sub>2</sub> to increase the surface properties of the HEAs [111].

#### **4.3 Laser surface alloying (LSA)**

This involves the direct injection or pre-placement of additional elements unto the surface of the substrate by a laser source. Rapid solidification occurs with the substrate maintaining its temperature while acting as a heat sink, still the composition of the surface changes [112]. Therefore, re-solidification and rapid quenching follow due to the temperature difference between the surface of the substrate and the treated surface zone. Zhang et al. [113] fabricated HEA coatings by LSA, and the HEA coating had a BCC solid solution phase with improved mechanical and corrosion properties. Jiang et al. [114] fabricated HEAs on a 304 stainless steel substrate and they stated that although the alloy had FCC and BCC phases, the BCC phase was more predominant. The authors also recorded a substantial increase in the hardness with good wear-resistant properties.

#### **4.4 Laser glazing**

This method produces a nanocrystalline layer or thin amorphous layer on the surface of the substrate, energy is absorbed into the surface which melts the HEAs coating/films to a certain depth with a laser beam and rapid solidification occurs. This process is achieved using a high power density at a short period enough to create the amorphous structure needed for surface modification [115].

### **5. Conclusion**

High-temperature properties of materials used for turbine engine applications are important for the reduction of fuel consumption, operating costs and pollution. Nickel-based superalloys are widely used due to its strength, resistance to degradation in oxidizing environments, toughness and density. However, Nickel superalloy

is not stable at elevated temperatures having a maximum service temperature of 649 °C, the superalloy at room temperature has a negative lattice misfit, poor thermal conductivity and difficult to machine. High Entropy Superalloys, with similar  $\gamma$  and  $\gamma'$  phases as the Nickel-based superalloys, shows high tensile strength than Inconel 617 and Alloy 800 H. The superalloy exhibits good oxidation resistance; have lower densities below 8 g/cm<sup>3</sup>, a positive lattice misfit and high yield strength compared to traditional nickel superalloys. Controlling the elemental compositional partitioning between the  $\gamma$ - $\gamma'$  in high entropy superalloys makes the thermal stability higher than conventional nickel superalloys and equimolar or near equimolar high entropy alloys. Therefore  $\gamma'$  precipitate strengthening of solid solution high entropy alloys to form High Entropy Superalloys is currently the most promising material for turbine engine applications. Laser surface modification treatments can be used as a protective mechanism for Superalloys.

## Acknowledgements

The authors will like to appreciate the National Laser Center (Laser Enabled Manufacturing Resource Group); Council for Scientific and Research (CSIR) and the Surface Engineering Research Laboratory; Tshwane University of Technology, Pretoria, South Africa for their scientific and technical support during this research.

## Author details

Modupeola Dada<sup>1\*</sup>, Patricia Popoola<sup>2</sup>, Ntombizodwa Mathe<sup>3</sup>, Samson Adeosun<sup>4</sup>, Sisa Pityana<sup>3</sup>, Olufemi Aramide<sup>2</sup>, Nicholas Malatji<sup>2</sup>, Thabo Lengopeng<sup>2</sup> and Afolabi Ayodeji<sup>2</sup>

<sup>1</sup> Chemical, Metallurgical and Materials Engineering, Tshwane University of Technology, Pretoria, South Africa

<sup>2</sup> Tshwane University of Technology, Pretoria, South Africa

<sup>3</sup> Council for Scientific and Industrial Research and Tshwane University of Technology, Pretoria, South Africa

<sup>4</sup> University of Lagos, Akoka, Lagos

\*Address all correspondence to: [dadadupeola@gmail.com](mailto:dadadupeola@gmail.com)

## IntechOpen

© 2021 The Author(s). Licensee IntechOpen. This chapter is distributed under the terms of the Creative Commons Attribution License (<http://creativecommons.org/licenses/by/3.0>), which permits unrestricted use, distribution, and reproduction in any medium, provided the original work is properly cited. 

## References

- [1] Boyce, M.P., *Gas turbine engineering handbook*. 2011: Elsevier.
- [2] Kaygusuz, K., *Sustainable development of hydroelectric power*. Energy sources, 2002. **24**(9): p. 803-815.
- [3] Langston, L.S., G. Opdyke, and E. Dykewood, *Introduction to gas turbines for non-engineers*. Global Gas Turbine News, 1997. **37**(2): p. 1-9.
- [4] Heywood, J.B., *Internal combustion engine fundamentals*. 2018: McGraw-Hill Education.
- [5] Bell, M. and T. Partridge, *Thermodynamic design of a reciprocating Joule cycle engine*. Proceedings of the Institution of Mechanical Engineers, Part A: Journal of Power and Energy, 2003. **217**(3): p. 239-246.
- [6] Cheng, C.-Y. and C.O.-K. Chen, *Power optimization of an irreversible Brayton heat engine*. Energy sources, 1997. **19**(5): p. 461-474.
- [7] Viteri, F. and R.E. Anderson, *Semi-closed brayton cycle gas turbine power systems*. 2003, Google Patents.
- [8] Walsh, P.P. and P. Fletcher, *Gas turbine engine*. 2005, Google Patents.
- [9] Li, Y. and P. Nilkitsaranont, *Gas turbine performance prognostic for condition-based maintenance*. Applied energy, 2009. **86**(10): p. 2152-2161.
- [10] Reed, R.C., *The superalloys: fundamentals and applications*. 2008: Cambridge university press.
- [11] Liu, C., et al., *Improved castability of directionally solidified, Ni-based superalloy by the liquid metal cooling process*. Metallurgical and Materials Transactions A, 2012. **43**(2): p. 405-409.
- [12] Wang, R.-Z., et al., *Creep-fatigue life prediction and interaction diagram in nickel-based GH4169 superalloy at 650 C based on cycle-by-cycle concept*. International Journal of Fatigue, 2017. **97**: p. 114-123.
- [13] Ganji, D.K. and G. Rajyalakshmi, *Influence of Alloying Compositions on the Properties of Nickel-Based Superalloys: A Review*, in *Recent Advances in Mechanical Engineering*. 2020, Springer. p. 537-555.
- [14] Akca, E. and A. Gürsel, *A review on superalloys and IN718 nickel-based INCONEL superalloy*. Periodicals of engineering and natural sciences, 2015. **3**(1).
- [15] Miracle, D.B., et al., *Refractory high entropy superalloys (RSAs)*. Scripta Materialia, 2020. **187**: p. 445-452.
- [16] Tsao, T.-K., et al., *High temperature oxidation and corrosion properties of high entropy superalloys*. Entropy, 2016. **18**(2): p. 62.
- [17] Yeh, A., et al., *Developing new type of high temperature alloys—high entropy superalloys*. International Journal of Metallurgical & Materials Engineering, 2015. **2015**.
- [18] Pint, B.A., K. Unocic, and S. Dryepondt. *Oxidation of superalloys in extreme environments*. in *7th International Symposium on Superalloy*. 2010.
- [19] Liu, X., et al., *Effects of Nb and W additions on the microstructures and mechanical properties of novel  $\gamma/\gamma'$ Co-V-Ti-Based superalloys*. Metals, 2018. **8**(7): p. 563.
- [20] Locq, D., et al., *Development of new PM superalloys for high temperature applications*. Intermetallics and superalloys, 2000. **10**: p. 52-57.

- [21] Graybill, B., et al. *Additive Manufacturing of nickel-based superalloys*. in *International Manufacturing Science and Engineering Conference*. 2018. American Society of Mechanical Engineers.
- [22] Walston, S., et al., *Joint development of a fourth generation single crystal superalloy*. 2004.
- [23] Perrut, M., et al., *High temperature materials for aerospace applications: Ni-based superalloys and  $\gamma$ -TiAl alloys*. *Comptes Rendus Physique*, 2018. **19**(8): p. 657-671.
- [24] Gessinger, G.H. and M. Bomford, *Powder metallurgy of superalloys*. *International Metallurgical Reviews*, 1974. **19**(1): p. 51-76.
- [25] Bewlay, B., et al., *Net-shape manufacturing of aircraft engine disks by roll forming and hot die forging*. *Journal of Materials Processing Technology*, 2003. **135**(2-3): p. 324-329.
- [26] Lavella, M., T. Berruti, and E. Bosco, *Residual stress analysis in Inconel 718 milled turbine disk*. *International Journal of Machining and Machinability of Materials*, 2008. **4**(2-3): p. 181-194.
- [27] Groh, J., et al. *Development of a new cast and wrought alloy (René 65) for high temperature disk applications*. in *Proceedings of the 8th International Symposium on Superalloy 718 and Derivatives*. 2014. John Wiley & Sons.
- [28] Pollock, T.M. and S. Tin, *Nickel-based superalloys for advanced turbine engines: chemistry, microstructure and properties*. *Journal of propulsion and power*, 2006. **22**(2): p. 361-374.
- [29] Ezugwu, E., J. Bonney, and Y. Yamane, *An overview of the machinability of aeroengine alloys*. *Journal of materials processing technology*, 2003. **134**(2): p. 233-253.
- [30] Reed, R., T. Tao, and N. Warnken, *Alloys-by-design: application to nickel-based single crystal superalloys*. *Acta Materialia*, 2009. **57**(19): p. 5898-5913.
- [31] Kennedy, R., *ALLVAC® 718PLUS™, superalloy for the next forty years*. *Superalloys*, 2005. **718**(706): p. 1-14.
- [32] Devaux, A., et al., *AD730TM-A new nickel-based superalloy for high temperature engine rotative parts*. *TMS Superalloys*, 2012. **911919**.
- [33] Thellaputta, G.R., P.S. Chandra, and C. Rao, *Machinability of nickel based superalloys: a review*. *Materials Today: Proceedings*, 2017. **4**(2): p. 3712-3721.
- [34] Flower, H.M., *High performance materials in aerospace*. 2012: Springer Science & Business Media.
- [35] Lehockey, E., G. Palumbo, and P. Lin, *Improving the weldability and service performance of nickel-and iron-based superalloys by grain boundary engineering*. *Metallurgical and materials transactions a*, 1998. **29**(12): p. 3069-3079.
- [36] Durand-Charre, M., *The microstructure of superalloys*. 2017: Routledge.
- [37] Sikka, V., et al., *Advances in processing of Ni3Al-based intermetallics and applications*. *Intermetallics*, 2000. **8**(9-11): p. 1329-1337.
- [38] Frank, R.B., C.G. Roberts, and J. Zhang. *Effect of nickel content on delta solvus temperature and mechanical properties of alloy 718*. in *7th international symposium on superalloy*. 2010.
- [39] Choudhury, I. and M. El-Baradie, *Machinability of nickel-base super alloys: a general review*. *Journal of Materials Processing Technology*, 1998. **77**(1-3): p. 278-284.

- [40] Gao, M.C. and D.E. Alman, *Searching for next single-phase high-entropy alloy compositions*. Entropy, 2013. **15**(10): p. 4504-4519.
- [41] Chatterjee, P., V.M. Athawale, and S. Chakraborty, *Selection of materials using compromise ranking and outranking methods*. Materials & Design, 2009. **30**(10): p. 4043-4053.
- [42] Chen, J., et al., *A review on fundamental of high entropy alloys with promising high-temperature properties*. Journal of Alloys and Compounds, 2018. **760**: p. 15-30.
- [43] Hummel, R.E., *Understanding materials science: history, properties, applications*. 2004: Springer Science & Business Media.
- [44] Cantor, B., et al., *Microstructural development in equiatomic multicomponent alloys*. Materials Science and Engineering: A, 2004. **375**: p. 213-218.
- [45] Ye, Y., et al., *High-entropy alloy: challenges and prospects*. Materials Today, 2016. **19**(6): p. 349-362.
- [46] Yeh, J.W., et al., *Nanostructured high-entropy alloys with multiple principal elements: novel alloy design concepts and outcomes*. Advanced Engineering Materials, 2004. **6**(5): p. 299-303.
- [47] Joseph, J., *Study of direct laser fabricated high entropy alloys*. 2016, Deakin University.
- [48] Kuehl, R.O. and R. Kuehl, *Design of experiments: statistical principles of research design and analysis*. 2000.
- [49] Wang, Y.P., B.S. Li, and H.Z. Fu, *Solid solution or intermetallics in a high-entropy alloy*. Advanced engineering materials, 2009. **11**(8): p. 641-644.
- [50] Gludovatz, B., et al., *A fracture-resistant high-entropy alloy for cryogenic applications*. Science, 2014. **345**(6201): p. 1153-1158.
- [51] Mishra, R.K. and R.R. Shahi, *Magnetic characteristics of high entropy alloys*. Magnetism and magnetic materials. IntechOpen, Rijeka, 2018: p. 67-80.
- [52] Senkov, O., et al., *Refractory high-entropy alloys*. Intermetallics, 2010. **18**(9): p. 1758-1765.
- [53] Hemphill, e.a., *Fatigue behavior of Al<sub>0.5</sub>CoCrCuFeNi high entropy alloys*. Acta Materialia, 2012. **60**(16): p. 5723-5734.
- [54] Tsao, T.-K., et al., *The high temperature tensile and creep behaviors of high entropy superalloy*. Scientific reports, 2017. **7**(1): p. 1-9.
- [55] Senkov, O.N., et al., *Development of a refractory high entropy superalloy*. Entropy, 2016. **18**(3): p. 102.
- [56] Chen, Y.-T., et al., *Hierarchical microstructure strengthening in a single crystal high entropy superalloy*. Scientific reports, 2020. **10**(1): p. 1-11.
- [57] Tsao, T.-K., A.-C. Yeh, and H. Murakami, *The microstructure stability of precipitation strengthened medium to high entropy superalloys*. Metallurgical and Materials Transactions A, 2017. **48**(5): p. 2435-2442.
- [58] Daoud, H., et al., *Microstructure and tensile behavior of Al 8 Co 17 Cr 17 Cu 8 Fe 17 Ni 33 (at.%) high-entropy alloy*. Jom, 2013. **65**(12): p. 1805-1814.
- [59] He, J., et al., *A precipitation-hardened high-entropy alloy with outstanding tensile properties*. Acta Materialia, 2016. **102**: p. 187-196.
- [60] Zhao, Y., et al., *Thermal stability and coarsening of coherent particles in a precipitation-hardened (NiCoFeCr)*

94Ti2Al4 high-entropy alloy. *Acta Materialia*, 2018. **147**: p. 184-194.

[61] Xiao, K., et al., *A scanning AC calorimetry technique for the analysis of nano-scale quantities of materials*. Review of Scientific Instruments, 2012. **83**(11): p. 114901.

[62] Wang, Z., et al., *Effect of coherent L12 nanoprecipitates on the tensile behavior of a fcc-based high-entropy alloy*. *Materials Science and Engineering: A*, 2017. **696**: p. 503-510.

[63] Gwalani, B., et al., *Stability of ordered L12 and B2 precipitates in face centered cubic based high entropy alloys-Al0.3CoFeCrNi and Al0.3CuFeCrNi2*. *Scripta Materialia*, 2016. **123**: p. 130-134.

[64] Borkar, T., et al., *A combinatorial assessment of Al<sub>x</sub>CrCuFeNi<sub>2</sub> (0 < x < 1.5) complex concentrated alloys: Microstructure, microhardness, and magnetic properties*. *Acta Materialia*, 2016. **116**: p. 63-76.

[65] Li, Y., et al., *Microstructure and elevated-temperature mechanical properties of refractory AlMo0.5NbTa0.5TiZr High Entropy Alloy fabricated by powder metallurgy*. arXiv preprint arXiv:1801.00263, 2017.

[66] Kai, W., et al., *The oxidation behavior of a Ni<sub>2</sub>FeCoCrAl<sub>0.5</sub> high-entropy superalloy in O<sub>2</sub>-containing environments*. *Corrosion Science*, 2019. **158**: p. 108093.

[67] Shafiee, A., et al., *Development and microstructural characterization of a new wrought high entropy superalloy*. *Metals and Materials International*, 2019: p. 1-12.

[68] Saito, T., et al., *Effect of Heat Treatments on the Microstructural Evolution of a Single Crystal High-Entropy Superalloy*. *Metals*, 2020. **10**(12): p. 1600.

[69] Zhang, L., et al., *Microstructure and mechanical properties of precipitation-hardened cast high-entropy superalloys*. *Materials Science and Technology*, 2020: p. 1-7.

[70] Belan, J., *GCP and TCP phases presented in nickel-base superalloys*. *Materials Today: Proceedings*, 2016. **3**(4): p. 936-941.

[71] Yeh, A.-c. and T.-K. Tsao, *High-entropy superalloy*. 2019, Google Patents.

[72] Zhang, J., et al., *The effect of lattice misfit on the dislocation motion in superalloys during high-temperature low-stress creep*. *Acta Materialia*, 2005. **53**(17): p. 4623-4633.

[73] Mughrabi, H., *The importance of sign and magnitude of  $\gamma/\gamma'$  lattice misfit in superalloys—with special reference to the new  $\gamma'$ -hardened cobalt-base superalloys*. *Acta materialia*, 2014. **81**: p. 21-29.

[74] Chawla, V., et al., *Corrosion Behavior of Nanostructured TiAlN and AlCrN Hard Coatings on Superfer 800H Superalloy in Simulated Marine Environment*. *Journal of Minerals and Materials Characterization and Engineering*, 2009. **8**(9): p. 693-700.

[75] Sidhu, T., et al., *Oxidation and hot corrosion resistance of HVOF WC-NiCrFeSiB coating on Ni- and Fe-based superalloys at 800 C*. *Journal of Thermal Spray Technology*, 2007. **16**(5-6): p. 844-849.

[76] Moody, N., et al., *Temperature effects on hydrogen-induced crack growth susceptibility of iron-based superalloys*. *Engineering Fracture Mechanics*, 2001. **68**(6): p. 731-750.

[77] Chung, D.-W., et al., *Effects of Cr on the properties of multicomponent cobalt-based superalloys with ultra high  $\gamma'$  volume fraction*. *Journal of Alloys and Compounds*, 2020: p. 154790.

- [78] Makineni, S., B. Nithin, and K. Chattopadhyay, *Synthesis of a new tungsten-free  $\gamma$ - $\gamma'$  cobalt-based superalloy by tuning alloying additions*. Acta Materialia, 2015. **85**: p. 85-94.
- [79] Peters, M., et al., *Titanium alloys for aerospace applications*. Advanced engineering materials, 2003. **5**(6): p. 419-427.
- [80] Clemens, H. and W. Smarsly. *Light-weight intermetallic titanium aluminides—status of research and development*. in *Advanced materials research*. 2011. Trans Tech Publ.
- [81] Wee, S., et al., *Review on Mechanical Thermal Properties of Superalloys and Thermal Barrier Coating Used in Gas Turbines*. Applied Sciences, 2020. **10**(16): p. 5476.
- [82] Goward, G.W., *Current research on the surface protection of superalloys for gas turbine engines*. JOM, 1970. **22**(10): p. 31-39.
- [83] Couturier, R. and C. Escaravage, *High temperature alloys for the HTGR Gas Turbine: Required properties and development needs*. 2001.
- [84] Sims, C.T., N.S. Stoloff, and W.C. Hagel, *superalloys II*. 1987: Wiley New York.
- [85] Zhu, S. and F. Wang, *Nanocrystalline, Enamel and Composite Coatings for Superalloys*, in *Production, Properties, and Applications of High Temperature Coatings*. 2018, IGI Global. p. 160-186.
- [86] Levi, C.G., *Emerging materials and processes for thermal barrier systems*. Current Opinion in Solid State and Materials Science, 2004. **8**(1): p. 77-91.
- [87] Goward, G., *Progress in coatings for gas turbine airfoils*. Surface and coatings technology, 1998. **108**: p. 73-79.
- [88] Galetz, M.C., *Coatings for superalloys*, in *Superalloys*. 2015, InTech. p. 277-298.
- [89] Chatterji, D., R. DeVries, and G. Romeo, *Protection of superalloys for turbine application*, in *Advances in corrosion science and technology*. 1976, Springer. p. 1-87.
- [90] Wu, C., et al., *Phase evolution and cavitation erosion-corrosion behavior of FeCoCrAlNiTi<sub>x</sub> high entropy alloy coatings on 304 stainless steel by laser surface alloying*. Journal of Alloys and Compounds, 2017. **698**: p. 761-770.
- [91] Zhang, S., et al., *Synthesis and characterization of FeCoCrAlCu high-entropy alloy coating by laser surface alloying*. Surface and Coatings Technology, 2015. **262**: p. 64-69.
- [92] Huang, C., et al., *Dry sliding wear behavior of laser clad TiVCrAlSi high entropy alloy coatings on Ti-6Al-4V substrate*. Materials & Design, 2012. **41**: p. 338-343.
- [93] Nahmany, M., et al., *Al<sub>x</sub>CrFeCoNi High-Entropy Alloys: Surface Modification by Electron Beam Bead-on-Plate Melting*. Metallography, Microstructure, and Analysis, 2016. **5**(3): p. 229-240.
- [94] Tian, Y., et al., *Research progress on laser surface modification of titanium alloys*. Applied Surface Science, 2005. **242**(1-2): p. 177-184.
- [95] Herd, R.M., J.S. Dover, and K.A. Arndt, *Basic laser principles*. Dermatologic clinics, 1997. **15**(3): p. 355-372.
- [96] Natto, Z.S., et al., *Comparison of the efficacy of different types of lasers for the treatment of peri-implantitis: a systematic review*. International Journal of Oral & Maxillofacial Implants, 2015. **30**(2).
- [97] Zhang, H., et al. *Synthesis and characterization of NiCoFeCrAl<sub>3</sub> high*

*entropy alloy coating by laser cladding*. in *Advanced Materials Research*. 2010. Trans Tech Publ.

[98] Zheng, B., Q.B. Liu, and L.Y. Zhang. *Microstructure and properties of MoFeCrTiW high-entropy alloy coating prepared by laser cladding*. in *Advanced Materials Research*. 2013. Trans Tech Publ.

[99] Ye, X., et al., *The property research on high-entropy alloy Al<sub>x</sub>FeCoNiCuCr coating by laser cladding*. Physics Procedia, 2011. **12**: p. 303-312.

[100] Guo, X., et al., *Corrosion behavior of aluminum in fluoride-containing discharge condition for excimer laser structure application*. Materials Research Express, 2019. **6**(10): p. 106519.

[101] Sharma, Y., et al., *Magnetic anisotropy in single-crystal high-entropy perovskite oxide La<sub>0.2</sub>Cr<sub>0.2</sub>Mn<sub>0.2</sub>Fe<sub>0.2</sub>Co<sub>0.2</sub>Ni<sub>0.2</sub>O<sub>3</sub> films*. Physical Review Materials, 2020. **4**(1): p. 014404.

[102] Dobbstein, H., et al., *Direct metal deposition of refractory high entropy alloy MoNbTaW*. Physics Procedia, 2016. **83**: p. 624-633.

[103] Nam, H., et al., *Effect of post weld heat treatment on weldability of high entropy alloy welds*. Science and Technology of Welding and Joining, 2018. **23**(5): p. 420-427.

[104] Rafique, M.M.A., *Additive Manufacturing of Bulk Metallic Glasses and their composites—Recent trends and approaches*.

[105] Ocelík, V., et al., *Additive manufacturing of high-entropy alloys by laser processing*. Jom, 2016. **68**(7): p. 1810-1818.

[106] Fan, Y., et al., *Effect of fiber laser welding on solute segregation and properties of CoCrCuFeNi high entropy*

*alloy*. Journal of Laser Applications, 2020. **32**(2): p. 022005.

[107] Rekha, M., N. Mallik, and C. Srivastava, *First report on high entropy alloy nanoparticle decorated graphene*. Scientific reports, 2018. **8**(1): p. 1-10.

[108] Xu, Y., et al., *Microstructure Evolution and Properties of Laser Cladding CoCrFeNiTiAl<sub>x</sub> High-Entropy Alloy Coatings*. Coatings, 2020. **10**(4): p. 373.

[109] Chen, C., et al., *Influences of laser surface melting on microstructure, mechanical properties and corrosion resistance of dual-phase Cr–Fe–Co–Ni–Al high entropy alloys*. Journal of Alloys and Compounds, 2020. **826**: p. 154100.

[110] Cai, Z., et al., *Microstructure and wear resistance of laser clad Ni–Cr–Co–Ti–V high-entropy alloy coating after laser remelting processing*. Optics & Laser Technology, 2018. **99**: p. 276-281.

[111] Ion, J., *Laser transformation hardening*. Surface engineering, 2002. **18**(1): p. 14-31.

[112] Manilal, K.M., et al., *A Review on Laser Surface Alloying*. International Research Journal of Engineering and Technology, 2017. **4**(03): p. 4.

[113] Zhang, S., et al., *Laser surface alloying of FeCoCrAlNi high-entropy alloy on 304 stainless steel to enhance corrosion and cavitation erosion resistance*. Optics & Laser Technology, 2016. **84**: p. 23-31.

[114] Jiang, P., et al., *Microstructure and Properties of CeO<sub>2</sub>-Modified FeCoCrAlNiTi High-Entropy Alloy Coatings by Laser Surface Alloying*. Journal of Materials Engineering and Performance, 2020: p. 1-10.

[115] Pawlowski, L., *Thick laser coatings: A review*. Journal of thermal spray technology, 1999. **8**(2): p. 279-295.